

Simulative study of SiO₂ atomic layer etching by controlled passivation time in capacitively coupled plasma

Zhong-Ling Dai^{1*}, Wan Dong¹, Yuan-Hong Song¹ and You-Nian Wang¹

¹Key Laboratory of Materials Modification by Laser, Ion and Electron Beams (Ministry of Education), School of Physics, Dalian University of Technology, Dalian 116024, P. R. China

*Corresponding author: daizhl@dlut.edu.cn

Abstract: With the development of microelectronics industry, especially as the critical dimension is now shrinking to sub 7 nm, plasma atomic layer etching (PALE) increasingly plays its irreplaceable role in realizing higher precision control of plasma etching. In our simulation we find that the aspect ratio dependent effect (ARDE) is obvious and the side wall etching is visible. By changing the passivation time at different etching cycles, the etching rate is able to be improved and the ARDE can be eliminated.

Keywords: Atomic layer etching (ALE), alternating CF₄ gas, CCP, Advanced Mixed Mode Pulsing technology (AMMP).

1. Introduction

Plasma etching is an essential step in the Micro-electromechanical Systems (MEMS) and Very Large Scale Integrated Circuits (VLSI)^[1,2] For decades, with industrial demand, microelectronic feature sizes continually shrink and structures become complex gradually, such as three dimension transistors and nanoscale device. The traditional Reactive Ion Etching (RIE)^[3] becomes difficult to meet the needs of critical dimension. As monolayer precision etching, true ALE can remove one layer of the target material within every cycle, and keep the side wall aligned and the bottom flattened, compared with the continuous etching.^[4]

The conception of the ALE had been proposed since the last century. A lot of research on ALE had been carried out recently experimentally and numerically in inductively coupled plasmas (ICPs) because ICP sources tend to generate large area and uniform plasma at low gas pressure.^[5] Sanbir S Kaler et al^[6] used Ar and alternating C₄F₈ plasma to realize the ideal ALE of SiO₂. However, the result showed that more or less than a monolayer may be removed per cycle in practice. Dominik Metzler et al^[7] removed silicon oxide from Si surface using CF₄ plasma and removed CF_x film using Ar/H₂ plasma. They indicated that Si surfaces is reoxidized with little oxygen during the Ar⁺ ion bombardment step of the ALE process. Masatoshi Kawakami et al^[8] studied the accumulation of CF_x film on the quartz window. The CF_x accumulation leads to a shift that the quartz window was etched. That result causes pollution of the etched gas and damage of quartz windows. Pollution of gas is also a cause of non-ideal etching morphology. The simulation of Chad M. Huard et al^[9] showed that the process of etching poly silicon has obvious self-limiting effect, by using the Ar and Cl₂ mixed gas. In addition, the ideal etching profile can be obtained by introducing the process of purge gas and the ARDE is eliminated. Chad M Huard et al^[10]

simulated the effect of plasma uniformity on ALE of Si in Ar and Cl₂/Ar plasmas. Their result shows that ALE processing can improve the uniformity in etch rate when operated in a saturated, ion starved regime. Keren J. Kanarik et al^[11] had been working on synergy in ALE. Researches show that the study of ion-neutral synergy can guide the directional ALE approach. The lower pressure ensures the anisotropy of ions, which may result in better profiles in high aspect ratio etching. Chad M. Huard et al^[12] presents the passivation time has an significant role in ALE of SiO₂. In addition, changing passivation time can improve the selectivity of SiO₂ over Si₃N₄. On account of high dissociation rate of ICP, more F and CF₃ radical particles are not conducive to the selectivity of etching in dielectric plasma etching of SiO₂. The study of CCP ALE had been developing gradually. Sonam D. Sherpa and Alok Ranjan^[13] demonstrated the quasi-atomic layer etching of silicon nitride in a CCP etch chamber. In their experiment, the saturated etch rate of one monolayer per cycle could not be attained. Based on atomic layer deposition (ALD), Gasvoda et al^[14] studied CCP ALE under the support of Mixed Mode Pulse (MMP) technology. They used Ar and C₄F₈ mixed gas to deposit CF_x film. In the etching step, using Ar⁺ to bombard CF_x film, in order to remove passivated SiO₂ layer. Takayoshi Tsutsumi Ryan et al^[15] studied CCP ALE differently than the last experiment of Gasvoda in the etching step. They used the O₂ plasma to oxidize the CF_x film. It is should be mentioned that the ion bombardment is too week to etch the CF_x film in the etching step. In the above two methods of CCP ALE, a step of purifying the gas is contained between passivation step and etching step. Personally, the vertical etching with ions in etching stage can show better etching morphology.

For CCP ALE, ARDE is obvious due to the decrease of neutral density in the passivation stage. In order to reduce the existing problems, we simulate the process of

CCP ALE by alternating CF₄ plasma with energetic Ar⁺ plasma beams. The article structure is as follows, a description of the computational model and reaction mechanism used for this study are in next section. Section 3 discusses the results and the conclusions are shown in Section 4.

2. Model description

2.1 Ar/CF₄ and Ar discharge model

In this paper, the fluid coupled by MC model is used to calculate the etching parameters. The structure is as follows, electron MC model receives the electric field from the fluid model.^[16] Then, the electron MC model transmits reaction rate coefficient and electron temperature to the fluid model. As a result of the fluid program can calculate the bulk and sheath automatically, the difference of the density between positive ions and the electron (or the sum of negative ions and electrons) is used for judging the position of sheath. Fluid model transfers the electric field and other parameters to ion MC step by step. Through the discharge model, the particle fluxes, ion energy distributions (IEDs)^[17] and ion angle distributions (IADs) are gotten. The reaction coefficients used are in **table 1**.

Table 1

Ar discharging model:

The main reactions in which electrons participate.

Reaction	Threshold (eV)	Reference
Ar+E→Ar ⁺ +2E	15.6	[18]
Ar+E→Ar ⁺ +E	11.56	[18]
Ar+E→Ar+E	0	[18]

Ar/CF₄ discharging model:

The main reactions in which electrons participate.

Reaction	Threshold (eV)	Reference
Ar+E→Ar ⁺ +2E	15.6	[18]
Ar+E→Ar ⁺ +E	11.56	[18]
Ar+E→Ar+E	0	[18]
CF ₄ +E→CF ₄ +E	0	[19]
CF ₄ +E→CF ₃ +F+2E	15.9	[19]
CF ₄ +E→CF ₂ +2F+2E	22	[19]
E+CF ₄ →2E+CF ₃ +F	27	[19]
E+CF ₄ →F+CF ₃ +E	34.5	[19]
E+CF ₄ →CF ₂ +F+E	16	[19]
CF ₄ +E→CF ₃ +2F+E	18	[19]
CF ₄ +E→CF ₂ +F+E	30	[19]
CF ₄ +E→F+CF ₃	15(Assumed value)	[19]

The other reactions:

Reaction	rate coefficient (cm ³ /s)	Reference
CF ₃ +CF ₄ →CF ₃ +CF ₄	4.0E-9	[20]
CF ₂ +CF ₄ →CF ₃ +CF ₃	1.88E-9	[20]
Ar ⁺ +CF ₄ →Ar+CF ₃ +F	7.0E-10	[20]
Ar ⁺ +CF ₄ →Ar+CF ₃	7.0E-10	[20]
Ar+CF ₃ →Ar ⁺ +CF ₃	1.0E-9	[20]
Ar ⁺ +F→Ar+F	5.0E-7	[20]
Ar ⁺ +CF ₃ →CF ₃ +Ar	4.0E-11	[20]
Ar ⁺ +CF ₂ →CF ₂ +Ar	4.0E-11	[20]
CF ₃ +CF ₄ →CF ₃ +CF ₄	1.8E-10	[20]
CF ₃ +CF ₃ →CF ₃ +CF ₃	1.71E-9	[20]
F+CF ₄ →CF ₄	2.0E-11	[20]
F+CF ₃ →CF ₃	1.8E-11	[20]
F+CF ₂ →CF ₂	9.9E-11	[20]
F ₂ +CF ₄ →CF ₃ +F	1.88E-14	[20]
F ₂ +CF ₃ →CF ₂ +F	8.3E-14	[20]
CF ₃ +F→CF ₃ +E	4.0E-10	[20]
CF ₃ +F→CF ₃ +E	3.0E-10	[20]
CF ₃ +F→CF ₃ +E	2.0E-10	[20]
F+F→F ₂	1.0E-10	[20]
CF ₃ +F→CF ₃ +F	3.00E-7	[20]
F+CF ₃ →CF ₃ +F ₂	8.7E-8	[20]
CF ₃ +F→CF ₃ +F	5.0E-7	[20]
CF ₃ +F→CF ₃ +F	9.80E-8	[20]
F ₂ +CF ₃ →F+CF ₃	1.0E-10	[20]
F+CF ₃ →F+CF ₃	1.0E-10	[20]
F ₂ +F→F ₂	4.0E-7	[20]
F ₂ +F→F ₂	4.0E-8	[20]

2.2 Trenching model

Cellular removal method coupled surface reaction MC method is used in the trenching model to obtain the etching profiles. The parameters obtained from the discharge model such as ions fluxes, neutral particle

densities, IEDs and IADs are taken into the trenching model.^[21] The ions and neutral particles are treated as pseudo particles. The pseudo particle is a random selection of density ratio. The energy and the angle of the pseudo particles which are impacting on the feature profile are randomly selected from their IEDs and IADs. Every pseudo particle is tracked until it hits a cell. In the cell, the generation of the reaction is determined by probability of reaction and the threshold value. If the condition is satisfied, the properties of the cell will change. In this work, we set the cell size to 0.35 nm. After every etching step and passivation step, the boundary between the space and the material is updated. **Table 2** shows the surface reactions that we considered in this simulation. The reactions include chemical reactions, physical sputtering and deposition reactions.

Table 2 Surface reaction mechanism

Species	Symbol
Ion	I ⁺
Polymerizing radical	CF _n
Photoelectron	R _e
polymer	P
Activated species	*
Gas phase species	g
Surface species	s
Hot neutral	h
Polymer adsorbed the fluoride	P-F
Assumed value	e
The adsorption rate	c
Sputtering yield coefficient (Argon is given, the others can be seen in the reference [21])	b

Reaction	A ₀	E _{th} (eV)	Reference
Physical sputtering			
I ⁺ + SiO ₂ → Si ₁ ⁺ + O ₂ I ⁺	0.0139 ^b	18	[21]
R _e + I ⁺ → CF ₃ ⁺ + I ₁ ⁺	0.2	100	[21]
Adsorption and chemical etching of neutral particles			
2F ₂ + Si ₁ → SiF ₂	0.2 ^c	...	[21]
2F ₂ + SiO ₂ → SiO ₂ F ₂	0.02	...	[21]
F ₂ + P ₁ → P-F	0.1	...	[21]
2F ₂ + SiO ₂ F ₂ → SiF ₄ ⁺ + O ₂ I ⁺	4.2e-6	...	[21]
2F ₂ + SiF ₂ → SiF ₄ ⁺	4.6e-4	...	[21]
CF ₃ + Si ₁ → SiCF ₃	0.1	...	[21]
CF ₃ + SiO ₂ → SiO ₂ CF ₃	0.9	...	[21]
CF ₃ + P ₁ → P-CF ₃	0.3	...	[21]
Ion-enhanced surface processes			
I ⁺ + SiF ₂ → SiF ₂ ⁺	0.629	4	[21]
I ⁺ + SiCF ₃ → SiCF ₃ ⁺	0.0361	E < 128	[21]
I ⁺ + SiO ₂ F ₂ → SiF ₄ ⁺ + O ₂ I ⁺	0.0454	4	[21]
I ⁺ + SiO ₂ CF ₃ → SiF ₄ ⁺ + CO ₂ I ⁺	0.0305	4	[21]
I ⁺ + SiO ₂ CF ₃ → Si ₁ + 2CO ₂ I ⁺	0.0361	E < 128	[21]
Generation and loss of polymer			
I ⁺ + P-F ₁ → CF ₃ ⁺ (ion-enhanced etching)	0.2	4	[21]
I ⁺ + SiCF ₃ → SiCF ₃ ⁺	0.0361	E < 128	[21]
CF ₃ + SiCF ₃ → SiCF ₃ + P ₁	0.8 ^c	...	[21]
I ⁺ + SiO ₂ CF ₃ → SiO ₂ CF ₃ ⁺ + P ₁	0.0361	E < 128	[21]
CF ₃ + SiO ₂ CF ₃ → SiO ₂ CF ₃ + P ₁	0.8 ^c	...	[21]

3.1 The etching parameters

3.1.1 Ar/CF₄ plasma

In this section, the average densities of the radio frequency period at the sheath boundary are showed in **Fig 1**. Six kinds of ions and six kinds of neutrals are considered in our simulation. The discharge condition is a parallel plate capacitively coupled Ar/CF₄ (90/10) mixed gas discharge at 550mTorr with a gap separation of 5.5cm by a 50V voltage source operated at 13.56MHz.

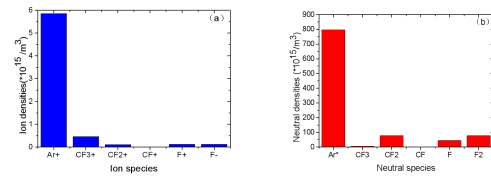


Fig 1 (a) ion densities;(b) neutral densities.

The the average IEDs and IADs of the radio frequency period at the substrate are exhibited in **Fig 2**. It is apparent that the IEDs (**Fig 2**.(a)) tends to be distributed at a low energy. Low energy ion is beneficial to selectivity and self-limiting of ALE.

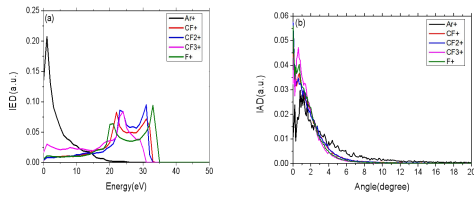


Fig 2 (a) Normalized IEDs that arrived at the substrate of Ar and CF₄ mixed gas in passivation stage; (b) Normalized IADs that arrived at the substrate of Ar and CF₄ mixed gas in passivation stage.

3.1.2 Ar plasma

The Ar⁺ energy distribution and angle distribution of the radio frequency period at the sheath boundary are given in **Fig 3**. A parallel plate capacitively coupled Ar discharge at 550mTorr with a gap separation of 5.5 cm is employed to calculate the discharge parameters. The voltage source is 150V operated at 13.56 MHz in this model. Under the same pressure conditions, the interpretation of results are similar to the previous one. The Radio Frequency (RF) periodic average density of Ar⁺ is $6.310442 \times 10^{15} \text{ m}^{-3}$ at the sheath boundary.

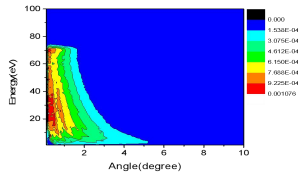


Fig 3 Normalized IEAD that arrived at the substrate of Ar gas in etching stage

3.2 Etching profiles

3.2.1 Etching profiles of the time evolution

In trenching model, the first 50 layers represent blank, and the 50 to 100 layers represent photoresist. The following layers are the etching material (In this simulation, it is silicon dioxide).

Fig 4 shows time evolution of the etching profiles. The working condition that the passivation stage is 1 second and the etching stage is 20 seconds is used. From the picture, as the etching depth increases, it is obvious that the sidewall etching are prominent. Owing to the pressure condition is relatively high, with the depth of trench increases, relatively greater angle ions tend to move to the side wall, which give rise to the sidewall etching.

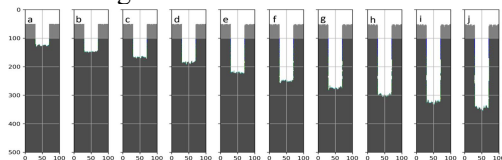


Fig 4 Etching profile of the time evolution (passivation time/etching time=1/20) a.25ALE cycles b.50ALE cycles c.75ALE cycles d.100ALE cycles e.150ALE cycle f.200 ALE cycles g.250ALE cycles h.300ALE cycles i.350 ALE cycles j.400ALE cycles

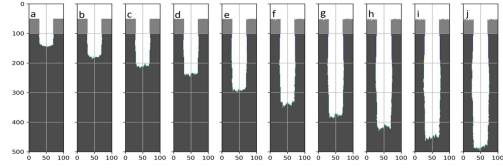


Fig 5 Etching profile of the time evolution (passivation time/etching time=3/20) a.25ALE cycles b.50ALE cycles c.75ALE cycles d.100 ALE cycles e.150ALE cycle f.200 ALE cycles g.250ALE cycles h.300ALE cycles i.350ALE cycles j.400ALE cycles

Compared to **Fig 6**, **Fig 7** that the passivation time is 4 seconds is given. From the picture, **Fig 7** showed the high etching rate than **Fig 6**. Whereas, the sidewall etching of **Fig 6** is not prominent comparatively. The reason for the difference of the etching rate is the reduction of the neutral groups in the passivation stage during the etch depth increase. The difference of the side wall etching is mainly due to the non-self-limiting in the passivation stage. From the surface reaction (table 2), passivation stage exists the case that the passivation layer is etched and SiO₂ is etched directly. Owing to the angle of passivation stage tend to be larger than the etching stage, the etching morphology shows severe side wall etching in **Fig 5**. In the industrial application, it is crucial that increase etching rate and improve side wall etching. This question is discussed in the next section.

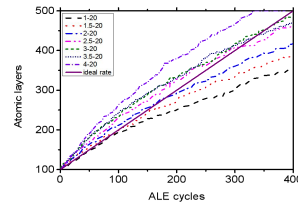


Fig 6 Etching rate in different passivation time (passivation time / etching time) (Magnitude: second))

As the period of ALE increases, the etching rate decreases gradually in the **Fig 6**. This phenomenon is the ARDE, which is mainly caused by the isotropic neutral atoms in the passivation stage gradually decreasing with the increase of etching depth. However, the etching rate increases slightly with the increase of passivation time. The longer process of the passivation shows that the etching rate exceeds the ideal etching rate. That can be explained from the surface reaction, in the passivation stage the ions can remove the passivation layer and the ions are able to remove silicon dioxide directly which lead to the non-self-limiting.

3.2.2 Changing the passivation time

With the increasing of etching precision, controlling etching rate of ALE becomes more and more important.

Here, the etching rate is improved by controlling the passivation time.

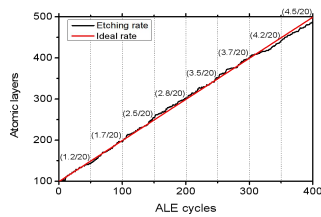


Fig 7 The passivation time is changed every 50 ALE cycles. (passivation time / etching time) (Magnitude: second))

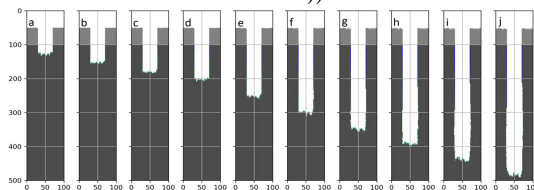


Fig 8 Etching profile of the time evolution after changing the passivation time at different etching cycle (a.25 ALE cycles b.50ALE cycles c.75ALE cycles d.100ALE cycles e.150ALE cycles f.200ALE cycles g.250ALE cycles h.300ALE cycles i.350ALE cycles j.400ALE cycles)

The passivation time in the cycle according to the etching rate is changed at the different trench depth. Etching rate is showed in **Fig 7** and the etching profiles is described in **Fig 8** after change the passivation time. In **Fig 7**, the passivation time/etching time changed every 50 cycles is 1.2/20, 1.7/20, 2.5/20, 2.8/20, 3.5/20, 3.7/20, 4.2/20, 4.5/20 respectively. Obviously, the condition of changing the passivation time is much better than the passivation time is only one form, for example the etching rate is closer to the ideal ALE etching rate and the etching profile is better than other the single passivation time. Simultaneously, changing the passivation time can partly eliminate the ARDE. All in all, with the increase of etching depth, the passivation time is increased. The influence of ion bombardment on the passivation layer in the passivation stage is reduced on the basis of meeting the requirement of passivation radicals.

4. Conclusions

To conclude, we simulated CCP ALE coupling one dimensional fluid/MC model with a trench model. From the figure of etching profile and etching rate, it is obvious that the etching profile demonstrates the severe side wall etching and the etching rate shows the ARDE. On account of pressure condition, the ion angle tend to large angle, the etching profile shows the non-ideal etching profiles--side wall etching. ARDE was mainly caused by the decreasing isotropic neutral gas as the etching depth increases. To some extent, when we change the passivation time at each 50 ALE cycles, the etching

profiles can be improved and the ARDE can be eliminated. In the long run, the selectivity and uniformity of ALE should be pay attention to and studied.

5. References

- [1] S.K.Tolpygo et.al. Journal of Physics: Conference Series. 97 (2008) 012227:1-9.
- [2] H.D.Ngo et.at. 2006, Journal of Physics: Conference Series. 34 (2006): 271-276.
- [3] M.Sekine. Applied Surface Science. 192 (2002) 270-298.
- [4] A.Agarwal et.al. J. Vac. Sci. Technol. A 27(1), Jan/Feb 2009: 27-37.
- [5] Lieberman.M.A, Lichtenberg. A. J. 1994, Principles of Plasma Discharges and Material Processing. New York, Wiley.
- [6]S.S. Kaler et.al. J. Phys. D: Appl. Phys. (2017) 50: 234001.
- [7] D.Metzler et.al. J. Phys. D: Appl. Phys. 50 (2017) 254006:1-9.
- [8] M.Kawakami et.al. J.Vac.Sci.Technol. A 34(4) Jul/Aug 2016 :1-5.
- [9] C.M.Huard et.al. 2017, Journal of Vacuum Science & Technology A:Vacuum, Surfaces, and Films 35, 031306.
- [10] C.M Huard et.al, J. Phys. D: Appl. Phys. 51 (2018) 155201:1-8.
- [11] K.J.Kanarik et.al. Journal of Vacuum Science & Technology A 35, 05C302 (2017):1-7.
- [12] C.M.Huard et.al. Journal of Vacuum Science & Technology A 36, 06B101(2018):1-24.
- [13] S.D.Sherpa et.al. Journal of Vacuum Science & Technology A: Vacuum, Surfaces, and Films 35, 01A102 (2017):1-6.
- [14] R.J.Gasvoda et.al. American Chemical Society. Applied Materials & Interfaces.2017, 9, 31067–31075.
- [15] T.T et.al.2016, J.Vac.Sci.Technol. A35,01A103.
- [16] Xi-Feng Wang et.al. Phys. Plasmas, 2017,24: 113503.
- [17] D.Kim et.al. IEEE TRANSACTIONS ON PLASMA SCIENCE, VOL. 30, NO. 5, OCTOBER 2002: 2048-2058.
- [18] A.V.Phelps et.al. Plasma Sources Sci. Technol. 8 (1999) R21–R44. Printed in the UK.
- [19] L. G. Christophorou et.al. Journal of Physical and Chemical Reference Data 25, 1341 (1996):1341-1388.
- [20] All the rate coefficients are given from CFD-ACE+ indexed file.
- [21] Sai-Qian Zhang et.al, Vacuum 99 (2014) 180-188.
- [22] E. Gogolidesa et.al. Journal of Applied Physics. 2000, 88(10): 5570-5584.
- [23]A.Sankaran et.al.J.Vac.Sci. Technol. A, Vol. 22,No 4, Jul/Aug (2004): 1260-1273.
- [24] Yukinobu.H et.al. Japanese Journal of Applied Physics. 1994, 33(4S): 2157..